Cysteine shotgun–mass spectrometry (CS-MS) reveals dynamic sequence of protein structure changes within mutant and stressed cells

Christine C. Krieger[a], Xiuli An[b], Hsin-Yao Tang[c], Narla Mohandas[b], David W. Speicher[c], and Dennis E. Discher[a,c,1]

[a]Molecular and Cell Biophysics Lab, University of Pennsylvania, Philadelphia, PA 19104; [b]New York Blood Center–Research Institute, New York, NY 10065; and [c]Systems and Computational Biology, The Wistar Institute, Philadelphia, PA 19104

Edited by Vann Bennett, Duke University Medical Center, Durham, NC, and approved March 18, 2011 (received for review December 17, 2010)

Questions of if and when protein structures change within cells pervade biology and include questions of how the cytoskeleton sustains stresses on cells—particularly in mutant versus normal cells. Cysteine shotgun labeling with fluorophores is analyzed here with mass spectrometry of the spectrin–actin membrane skeleton in sheared red blood cell ghosts from normal and diseased mice. Sheared samples are compared to static samples at 37 °C in terms of cell membrane intensity in fluorescence microscopy, separated protein fluorescence, and tryptic peptide modification in liquid chromatography–tandem mass spectrometry (LC-MS/MS). Spectrin labeling proves to be the most sensitive to shear, whereas binding partners ankyrin and actin exhibit shear thresholds in labeling and both the ankyrin-binding membrane protein band 3 and the spectrin–actin stabilizer 4.1R show minimal differential labeling. Cells from 4.1R-null mice differ significantly from normal in the shear-dependent labeling of spectrin, ankyrin, and band 3: Decreased labeling of spectrin reveals less stress on the mutant network as spectrin dissociates from actin. Mapping the stress-dependent labeling kinetics of α- and β-spectrin by LC-MS/MS identifies Cys in these antiparallel chains that are either force-enhanced or force-independent in labeling, with structural analyses indicating the force-enhanced sites are sequestered either in spectrin's triple-helical domains or in interactions with actin or ankyrin. Shear-sensitive sites identified comprehensively here in both spectrin and ankyrin appear consistent with stress relief through forced unfolding *followed by* cytoskeletal disruption.

cysteine labeling | repeat domain | conformation | oxidation state | mechanotransduction

The folding and association states of the many proteins *within* a cell might never be assessed by high-resolution methods of diffraction or NMR applied to the cell, but for structural proteins of the cytoskeleton such questions are likely central to understanding stress responses and probably signal transduction. The simplest mammalian cell, the RBC, possesses a well-elaborated membrane skeleton (1) assembled from α- and β-spectrin plus F actin with proteins such as 4.1R (2) helping to stabilize the network and ankyrin (3) helping to attach the network to the membrane (Fig. 1*A*). However, it is unclear whether these proteins dissociate and/or unfold as the cytoskeleton is stressed in blood flow. Deeper insight is needed to explain, for example, the strong effects of point mutations that are sometimes distal to protein interaction sites (4). To begin to address such issues we have developed a method to map dynamically exposed cysteines in proteins of intact cells that are stressed mechanically, thermally, or by drugs (5). Cys is relatively hydrophobic, which means that it is frequently buried—wholly or partially—in protein folds as well as in protein–protein interfaces, but the thiol in cysteine is also highly reactive. Fluorescent dyes allow "shotgun" labeled cells to be imaged and the labeled proteins to be both quantified and site-by-site analyzed using Cys shotgun–mass spectrometry (CS-MS). Controlled stressing of human RBC membranes by fluid shear stresses at levels similar to in vivo blood flow stresses (up to 1–2 Pa) has thus revealed stress-enhanced Cys labeling at 37 °C, with forced unfolding of some of the dozens of three-helix repeat domains (Fig. 1*B*) (5). Whether other membrane skeleton proteins contribute and show stress-enhanced labeling was not previously addressed.

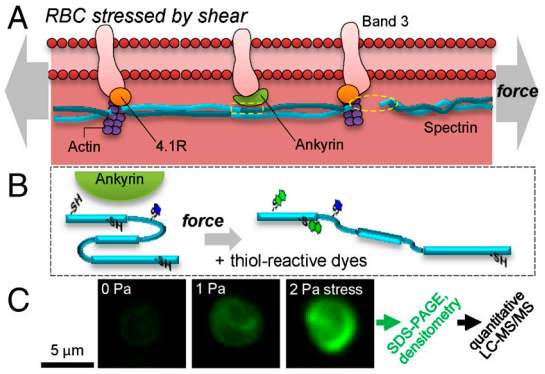

Fig. 1. Shear stress response of red cell membrane cytoskeleton as detected by Cys-shotgun labeling. (*A*) Shearing of the membrane tends to stretch the spectrin–actin network, perhaps from a slack or curved state, with possible stressing of attachment proteins protein 4.1R and ankyrin as well as integral membrane proteins such as band 3. (*B*) Forces can either unfold spectrin repeats or dissociate spectrin from ankyrin (dashed box) and/or actin (dashed oval). Fluorescent thiol probes loaded into cells react with solvent exposed (blue dye) and newly exposed cysteines (green dye), revealing changes in tertiary and quaternary structure. (*C*) Stress-dependent labeling of the membrane can be visualized and measured in intact RBC ghosts that were labeled for the same duration at 37 °C but exposed to various physiological levels of shear stress (units of Pascal: Pa).

Denaturation studies of purified spectrin decades ago showed spectrin repeats unfold collectively and cooperatively only for $T \gg 37$ °C (6), but in more recent studies in which almost every spectrin repeat was recombinantly expressed, more than a third of the domains unfolded at or below 37 °C (7). Single molecule experiments have shown that spectrin domains—independent of melting temperature—unfold at relatively low force compared to other proteins such as titin (8), and the forced unfolding can cooperatively propagate through multiple domains (9, 10) with significant perturbations in some mutant spectrins (11). In addition, RBC ghosts with spectrin interacting fragments entrapped inside show shear-enhanced incorporation into the cytoskeleton (12). This raises the question of how much dissociation occurs

Author contributions: C.C.K. and D.E.D. designed research; C.C.K. performed research; X.A., H.-Y.T., N.M., and D.W.S. contributed new reagents/analytic tools; C.C.K. and D.E.D. analyzed data; and C.C.K. and D.E.D. wrote the paper.

The authors declare no conflict of interest.

This article is a PNAS Direct Submission.

[1]To whom correspondence should be addressed. E-mail: discher@seas.upenn.edu.

This article contains supporting information online at www.pnas.org/lookup/suppl/doi:10.1073/pnas.1018887108/-/DCSupplemental.

under stress relative to unfolding of spectrin's many repeat domains—especially in normal versus mutant cells, such as from 4.1R-null mice, which have mechanically fragile RBCs (13).

Results and Discussion

Stress Enhances Cys Labeling of Spectrin in Mouse Cell Membranes, but Labeling Is Low in 4.1R-Null Mutants. Fluorescence microscopy shows that RBC membranes from normal mice have a higher intensity when labeled at higher shear stress (Fig. 1*C*). RBCs were lysed to remove hemoglobin and its highly reactive cysteines (14), and then Cys reactive dyes were entrapped. Blue dye [N-(Iodoacetaminoethyl)-1-naphthylamine-5-sulfonic acid (IAEDANS)] was added first to label Cys exposed on the surfaces of proteins, thus resulting in a "background" signal. Green dye [N-(4,4-difluoro-1,3,5,7-tetramethyl-4-bora-3a,4a-diaza-s-indacene-2-yl) iodoacetamide] (BODIPY) was then added with the aim of separately labeling stress-exposed sites, and the resealed ghosts were then quickly split and either held "static" at 37 °C or else sheared at 37 °C at physiological stresses (<2 Pa) in a standard stress-controlled fluid-shearing device for up to 60 min. Labeling differences with the second dye (e.g., BODIPY) are most apparent at 30–60 min, consistent with previous studies (5).

To identify membrane proteins labeled at a specific time and stress and to quantify the labeling per mass, SDS-PAGE gels were run with various loads of solubilized membranes and then imaged in both fluorescence and after Coomassie staining for protein mass (Fig. 2*A*). Cysteines are underutilized in many cytoskeletal proteins, occurring in spectrin, for example, at only one to two per

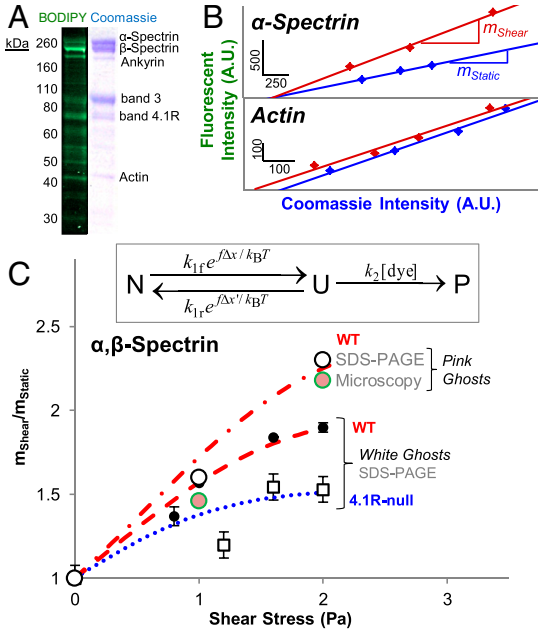

Fig. 2. Spectin labeling depends on stress and on 4.1R. (*A*) Images of an SDS-PAGE-separated RBC ghost membrane lysate in fluorescence with BODIPY labeling or after staining with Coomassie dye, showing considerable labeling of many cytoskeletal proteins. (*B*) Fluorescence and Coomassie intensity of individual bands was quantified by densitometry for different amounts of the same lysate and then fit to a line ($R^2 > 0.95$). The ratio of slopes, (m_{shear}/m_{static}), for a given shear stress and time (60 min), shows that α-spectrin labeling is shear-enhanced, whereas actin labeling is shear-independent. (*C*) The labeling ratio for α,β-spectrin increases with shear stress, and the results fit to fLL reaction kinetics for a force-accelerated transition from native to unfolded (*Inset*; see *SI Text*) shown as dashed lines. Densitometry of spectrin from WT pink ghosts (open circles: WT), shows the same stress-enhanced fluorescence labeling as that measured by microscopy of intact pink ghosts (pink circles). With white ghosts, labeling of spectrin from normal cells, black dots, exceeds the labeling of spectrin from 4.1R-null cells.

approximately 100 amino acids (versus random usage of approximately 5%), but the proteins are nonetheless labeled robustly by the fluorescent dyes when compared to Coomassie stain. Densitometry of both signals at the various lysate concentrations (Fig. 2*B*) provides a specific labeling level as a slope m for each stress condition, i.e., m_{shear} or m_{static}. A ratio $(m_{shear}/m_{static}) > 1$ for spectrin was found for all shear stresses tested and indicates force-enhanced labeling, whereas $(m_{shear}/m_{static}) = 1$ was found for actin at low stress (see below). Note that static labeling is nonzero and depends on the particular dye, but such effects are common to both static and shear samples. Equal labeling of α-spectrin and β-spectrin (within 5%) is consistent with an antiparallel arrangement of molecular "springs" being equally stressed.

With increasing shear stress (for 60 min at 37 °C), spectrin's labeling ratio increases (Fig. 2*C*). As with white ghosts, pink ghosts with approximately 20% of physiological hemoglobin show increased BODIPY labeling with shear stress, both for spectrin separated by SDS-PAGE and in fluorescence imaging of the sheared ghosts (after a final hemolysis). Ghost membranes and spectrin bands were labeled about twice as much after being stressed at 2 Pa versus 1 Pa, with relatively tight error bars. Additional labeling of pink ghosts perhaps reflects the enhanced viscosity and stress in such ghosts.

The 4.1R-null cells mutant show decreased spectrin labeling relative to the various wild-type samples, and the labeling appears nonlinear and almost step-like. The maximum labeling at high stress is also only 50% higher than static cell labeling. 4.1R therefore has an important effect on stress-dependent network dynamics.

Shear-enhanced labeling of spectrin was fit to a force-dependent Linderstrom–Lang (fLL) reaction (Fig. 2*C*, *Inset*), which models a stress-dependent shift in equilibrium from native folded (or associated) domains to unfolded (or dissociated) domains followed by irreversible labeling of exposed cysteines. The fLL merely assumes one overall process with respect to Cys labeling, although some or all of the molecules could start with some slack, compressed, or bent. Spectrin labeling in normal mouse RBCs fits very well to the fLL equation with just two adjustable parameters ($R^2 = 0.98$; see Table S1) plus parameters already used for fits of normal human RBCs under stress (5) and based in part on single molecule AFM studies of forced unfolding (9–11). Although step-like data for 4.1R-null cells do not fit very well to the fLL equation ($R^2 = 0.76$), which suggests additional processes, a lower unfolding rate for these cells also suggests less stress sustained by spectrin. Forced and rapid dissociation of spectrin from actin seems plausible because the spectrin–actin association in the absence of 4.1R is known to be very weak at $K_d \sim 10$ μM (15, 16). If 4.1R normally keeps spectrin bound to actin when the membrane is stressed, then spectrin can be stretched and unfolded; but if 4.1R is missing, then spectrin will detach from actin when the membrane is stressed and spectrin stretching and unfolding will be less likely. 4.1R-null cells also have less spectrin, actin, and other membrane proteins (13, 17), and so the fewer cross-links in these cells would tend to be more rapidly stressed and dissociated, thereby relaxing spectrin before much labeling occurs. It is nonetheless conceivable that much smaller shear stress than used here might cause more unfolding and labeling of spectrin in 4.1R cells than in normal cells, but smaller stresses would also give less labeling per protein and thus be much more difficult to measure.

Stress-Enhanced Labeling of Actin and Ankyrin Exhibits a Threshold. Simultaneous exposure of all proteins to thiol-reactive dye allows a comparison of any stress-dependent changes of other cytoskeletal proteins to spectrin. Although stress-dependent labeling of spectrin is essentially linear, stress-enhanced labeling of actin and ankyrin (Fig. 3*A*) occurs only at stress >0.8 Pa, suggesting protein dissociation at high force. Reaction rates for a concentra-

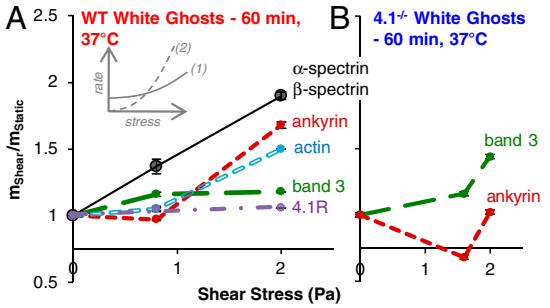

Fig. 3. Ankyrin and actin labeling exhibit a shear threshold that depends on 4.1R. (*A*) With normal ghosts, a low shear stress of 0.8 Pa primarily causes force-enhanced labeling of spectrin, but at a higher shear stress of 2.0 Pa, ankyrin and actin also show considerable stress-enhanced labeling, whereas band 3 and 4.1R show little to no stress-enhanced labeling. (*B*) With 4.1R-null ghosts, band 3 labeling is stress-enhanced, whereas ankyrin labeling is not. Actin was not be analyzed because actin levels in 4.1R-null cells are lower than in wild type.

tion n are generally accelerated by stress σ as rate $= n\ k_o \exp(\sigma/\sigma_o)$, with both the unstressed rate k_o and the stress scale σ_o being characteristic of each reaction (unfolding or dissociation). For competing reactions, if reaction-(1) has a high k_o but large σ_o while reaction-(2) has a low k_o and small σ_o, then there is an understandable transition from reaction-(1) dominated to reaction-(2) dominated at high stress (Fig. 3*A*, *Inset*). Here, reaction-(1) represents up to $n_1 = 2 \times 37 = 74$ unfolding reactions for spectrin tetramer domains per ankyrin dissociation reaction-(2) (i.e., $n_2 = 1$), and if one assumes for simplicity that all of the k_o's are the same, then the net rates of unfolding versus dissociation are equal when

$$\text{rate}_1/\text{rate}_2 \approx (n_1/n_2)\ \exp(\sigma/\sigma_{o1} - \sigma/\sigma_{o2}) = 1.$$

This occurs at $\sigma \sim 2$ Pa (Fig. 3*A*), giving $\sigma_{o2} \approx \sigma_{o1}/(1 + 2.1\sigma_{o1})$. The stress-enhanced rate of labeling any one domain in Fig. 3*A* is also estimated as $\exp(2\ \text{Pa}/\sigma_{o1}) \approx 2$, and so $\sigma_{o1} \approx 2$ Pa and $\sigma_{o2} \approx 0.4$ Pa. Ankyrin dissociation from spectrin might thus be more stress-sensitive (low σ_o) but *many spectrin domains unfold* first. Entropy thus dominates.

In contrast to large labeling changes in spectrin, actin, and ankyrin, band 3 shows only slight shear-enhanced labeling at low and high stress (+15%) whereas 4.1R shows no significant force-dependent labeling. Band 3's large cytoplasmic tail interacts with the spectrin network through ankyrin and possesses Cys that might be stress-exposed (17, 18), whereas 4.1R is a globular stabilizer of spectrin–actin and a connector of F-actin protofilaments to the membrane. Spectrin thus seems stretched and unfolded at low stress, whereas high stress dissociates a fraction of spectrin–actin and also extends ankyrin with dissociation of a fraction of ankyrin from spectrin and/or band 3.

Loss of 4.1R limits force-enhanced labeling of ankyrin to $(m_{\text{shear}}/m_{\text{static}}) = 1.0$ at the highest shear stress of 2 Pa (Fig. 3*B*). Without 4.1R, spectrin dissociation from actin at low stress would certainly reduce the tension on spectrin and not only minimize force-enhanced unfolding and labeling of spectrin as observed (Fig. 2*C*) but would also minimize stress on ankyrin. Remarkably, a somewhat lower shear stress of 1.6 Pa leads to less labeling of ankyrin than in static 4.1R-null cells: $(m_{\text{shear}}/m_{\text{static}}) < 1.0$. Cys labeling in static cells is dominated by sites on the protein surface and also perhaps involves buried sites that are exposed at a basal rate dictated by a basal cytoskeletal stress in the RBC membrane (19). With 4.1R-null RBCs, the shear-enhanced spectrin dissociation from actin—which is decreased in abundance (17)—could therefore reduce the net tension on the ankyrin–spectrin interface to levels below static levels. At the same time, band 3 in the 4.1R-null cells at the highest shear exhibits significantly more stress-enhanced labeling than wild-type cells; previous work with 4.1R-null cells had indeed suggested that band 3 undergoes a conformational change in the absence of 4.1R (17). The exact nature of this change and its shear sensitivity needs further study, especially at small stresses, but all of the molecular responses here are distinct from normal cells.

Cys Shotgun Mass Spectrometry Kinetic Maps: Half the Sites Exhibit Force-Dependent Labeling. Cys adducts of IAEDANS and monobromobimane (mBBr) have both been shown to survive the ionization and fragmentation processes of tandem mass spectrometry (5) (BODIPY does not remain intact), and so we used both dyes to identify and quantify tryptic peptides of spectrin that are labeled in sheared mouse cell membranes. Roughly similar in size to a tryptophan side chain, the dyes label buried Cys without greatly perturbing the refolding of proteins (5). Labeling under static conditions was compared to labeling at moderately high shear stress of 1.5 Pa for $t = 30$ and 60 min, and unreacted Cys in all samples (no reaction went to completion) were capped with iodoacetamide (IAM), providing a means to normalize dye results. IAEDANS was entrapped in ghosts first in an attempt to differentially label fast-reacting Cys on the protein surfaces even though the efficiency of labeling and/or MS detection of this dye is low. Lysates were separated by SDS-PAGE and spectrin bands were excised, trypsinized, and run through liquid chromatography–tandem mass spectrometry (LC-MS/MS). Sequence coverage was about 76% for α-spectrin and 68% for β-spectrin; 17 cysteines were detected, with 13 located in repeat domains, and 3 of these were predicted to be surface exposed (Table S2).

Force-enhanced labeling for individual tryptic peptides was determined from normalized ion fluxes in the first MS as the ratio for IAEDANS, $\Phi_{\text{time}} = [(\text{Cys-IAEDANS})/(\text{Cys-IAM})]$, or else as φ_{time} for mBBr, with $(\Phi,\varphi) \geq 1.25$ appearing to be a sound criterion for force-enhanced labeling. Even at moderately high shear stress, only two Cys appear shear sensitive at 30 min in LC-MS/MS analyses, whereas nearly half of the Cys show force-enhanced labeling at 60 min (Fig. 4*A*). The average (Φ, φ)-values for force-enhanced Cys labeling were fitted to the fLL equation

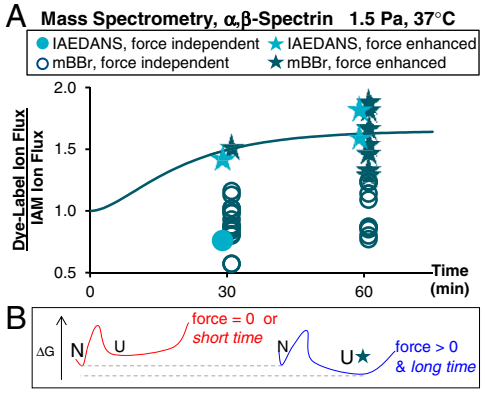

Fig. 4. Cys shotgun–mass spectrometry labeling kinetics identify force-enhanced and force-independent sites. (*A*) Ion fluxes in MS of dye-labeled spectrin peptides were normalized to IAM-modified peptides in the same sample and represented by Φ and φ for IAEDANS and mBBr modified peptides, respectively. The fLL curve was generated using the same parameters as in the WT-white ghost analysis (Fig. 2*C* and Table S1) and used to define the cutoff for force-enhanced labeling, $\Phi,\varphi \geq 0.25$. This cutoff was chosen such that average Φ, φ for force-enhanced cysteines fit to the fLL curve ($R^2 = 0.97$). Starred points represent cysteines with force-enhanced labeling. After 30 min of moderate shear, only two of the detected cysteines showed significant force-enhanced labeling, whereas at 60 min, about half of the cysteines showed force-enhanced labeling. (*B*) Representative schematic of the fLL-based free energy landscape for force-sensitive domains. At zero stress or short times, unfolding and labeling of such domains is unlikely, whereas force and time both enhance labeling.

(Fig. 4*A*) using the same parameters as for spectrin in normal cells (Fig. 1*C*). This indicates that the stress-dependent average labeling measured by densitometry of SDS-PAGE can also be quantified by LC-MS/MS at the level of individual domains.

Tabulation of all detected labeled peptides with (Φ, φ)-values in Table S2 shows that domain locations as well as predicted accessibilities are highly variable. Solvent accessibility of Cys located within repeat domains was predicted by heptad position within the helices (20) (Fig. S1), with five sites showing force-enhanced labeling at 60 min. These domains thus seem likely to have unfolded during shear, but two Cys that were predicted to be solution-exposed also show force-enhanced labeling at 60 min. Overall accuracy of the shear/static ratio measurements by LC-MS/MS is evident in the fact that there are essentially no ratios much less than 1.0, and also only some ratios increase with time.

Labeling Kinetics at Junctional Cys Reveals Different Binding Strengths in Spectrin Associations. Kinetic mapping of labeled peptides by LC-MS/MS shows that two Cys that are force-exposed at 30 min under high shear are located at or near sites of protein–protein interaction (Fig. 5*A*). Cys β1883 is directly adjacent to the spectrin–ankyrin-binding site, whereas Cys α473 is located across from the spectrin tetramer interface, which is a couple of repeats distal to the spectrin–ankyrin-binding site. Force exposure of both cysteines correlates with the increased labeling of ankyrin at high shear (Fig. 3*A*).

Cysteines near the spectrin–actin interaction—in either the CH1 domain (β112) or in repeat 21 of α-spectrin (α2155)—show shear-enhanced labeling only at 60 min in these normal cell membranes (Fig. 5*B*). According to densitometry results, both ankyrin and actin show force-enhanced labeling at high stress (60 min), but spectrin binding to the actin–4.1R complex is about 50-fold stronger than the cited binary interactions (15, 16) and therefore stronger than spectrin–ankyrin binding ($K_d = 10^{-7}$ M) (21), which makes it likely that ankyrin dissociates first from the spectrin network. Cys α2155 was predicted to be buried within repeat 21, but its labeling seems indicative of high stress at the spectrin–actin junction.

Cysteine homology between mouse and human spectrins is striking, with past studies revealing Cys exposure in several sites seen also in mouse, including α222, α1877, and β595 (Fig. 5*C*). Cys in human repeat β15 also shows increased labeling in shear, which implicates dissociation from ankyrin, and shear-enhanced labeling of human ankyrin was indeed significant if small in previous studies of human membranes (5). The same cited studies did not reveal a significant shear dependence to actin labeling, consistent with cysteines in human α-spectrin repeat 21 and β-spectrin's CH1 domain showing no shear enhancement. Therefore, in human RBCs and likely in mouse RBCs, spectrin dissociation from actin is uncoupled from forced dissociation of spectrin from ankyrin.

Several additional differences exist in the labeling patterns of human and mouse spectrins, which may argue that the transmission of force is somewhat species dependent. Cys α473 and β1544 show shear-enhanced labeling, whereas the human homologues do not. Cys α1248 in repeat α12 is not homologous to the human cysteine in that repeat, but although both are predicted to be buried, shear-enhanced labeling is seen only in human, which suggests that repeat α12 unfolds in human RBCs and perhaps not in mouse. Cys β1159 is located in the linker between repeats β8-9, based on a crystal structure (22), and labeling of this site appears independent of stress in mouse but strongly stress-dependent in humans (5). Sequence differences in the linker region could have distinct effects on linker flexibility and Cys exposure (Fig. S2*A*).

Cys Labeling in Relation to Atomic Models of Interaction Domains. Homology models of mouse domains were made based on exist-

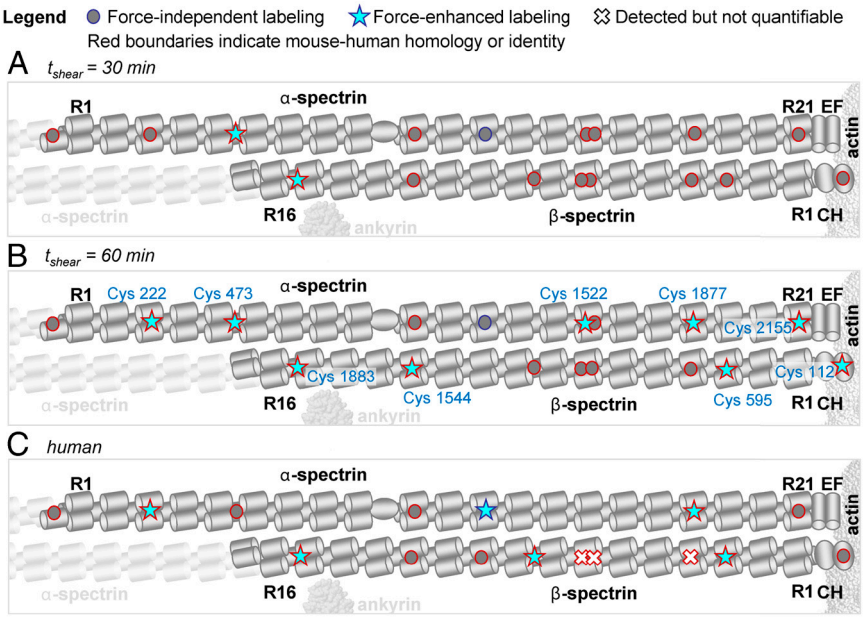

Fig. 5. Kinetic maps of labeled Cys detected by mass spectrometry. Ghosts were sheared at a moderate shear stress (1.5 Pa), below the threshold of ankyrin and actin dissociation but high enough to expect significant spectrin unfolding (Fig 2*C*). The force-enhanced labeling of individual cysteines was assessed via the ion-flux ratio of modified/unmodified peptides (Tables S2 and S3). In this schematic, repeat domains are depicted as three-cylinder bundles. All cysteines detected by mass spectrometry are represented by gray circles (force-independent labeling), blue stars (force-enhanced labeling), or white x's (unquantifiable). White x's represent cases where only modified cysteines were detected, and the modified/unmodified ratio could not be calculated. Red outlines mark cysteines that are homologous with cysteines in human spectrin. (*A*) After 30 min of moderately high shear stress (1.5 Pa), only Cys located near the spectrin–ankyrin junction show force-enhanced labeling (stars). (*B*) After 60 min, Cys near the spectrin–actin junction as well as Cys buried within repeat domains show force-enhanced labeling. At both time points, there are also many Cys for which measurements show labeling is force-independent. (*C*) Many of the cysteines detected here in mouse spectrins are homologous to the Cys detected in previous studies of human RBCs (6), with some disparities likely due to sequence and/or structure differences. Amino acids and repeat assignments were made according to Uniprot files P08032 (mouse α-spectrin), P15508 (mouse β-spectrin), P02539 (human α-spectrin), and P11277 (human β-spectrin).

ing crystal structures, suggesting that Cys β112, β1883, and α473 are all partially exposed to solution so that some labeling is expected even in static samples. Cys β112 is within helix E of the CH1 domain and is very close to the spectrin–actin interface (Fig. 6*A* and Fig. S2*B*). Dissociation from actin is expected to greatly increase the labeling efficiency at least because of decreased steric hindrance. Although it is not yet known whether 4.1R possesses any cryptic Cys that are sequestered within folds or binding interfaces, this protein shows no stress-enhanced labeling but is certainly labeled under all conditions.

The thiol in Cys β1883 is directed toward the hydrophobic core of this spectrin repeat and is located at the end of a domain involved in spectrin–ankyrin binding (23) (Fig. 6*B* and Fig. S2*C*). Site-directed mutagenesis in the large and unusual kink between β-repeats 14–15 has suggested a *mechanosensitive*, conformationally plastic binding site for ankyrin with possible relations to domain linker mutations in hemolytic anemias (24). Increased labeling of Cys β1883 in stressed cells here might thus reflect enhanced accessibility with conformational changes at moderate shear stress (1.5 Pa) or perhaps it indicates forced dissociation from ankyrin, consistent with the 5-fold higher stress sensitivity (see σ_o estimates above). At about the same stress, the 4.1R null cells showed reduced labeling of ankyrin (Fig. 3*B*), which might indicate that spectrin binding to (or shielding by) ankyrin is enhanced by relaxation of cytoskeletal tension in these cells containing decreased amounts of ankyrin and band 3 (17). Alternatively, small structural changes in the complex during shear could allow thiol probes greater access to a given cysteine without the dissociation or outright domain unfolding.

Cys α473 is located on a helix that is part of the proximal tetramerization interface between α- and β-spectrin (Fig. 6*C*). It is on the opposite side of the helix involved in the interaction (25), and so labeling of this residue does not necessarily imply dissociation of the spectrin tetramer. However, force-enhanced labeling of this site could indicate extra stress exerted at this junction when cells are sheared.

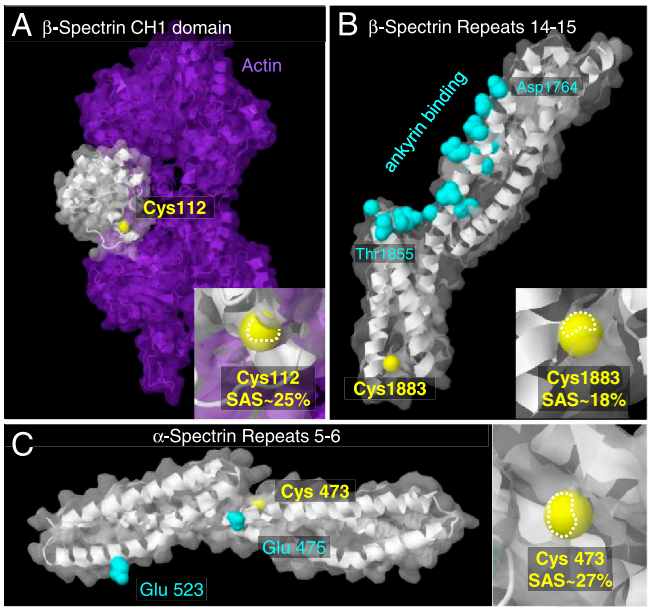

Fig. 6. Force-enhanced labeling around spectrin binding sites. Homology models of mouse spectrin domains were made based on existing crystal structures (see *Materials and Methods*) and used to estimate the spatial relationship between detected Cys and previously studied, functionally important residues. Secondary structure is represented in ribbon form, and the translucent surface represents the solvent accessible surface (SAS). Thiol groups of cysteines of interest are shown yellow in spacefill with %-SAS indicated; 0% would be a buried Cys. (*A*) The CH1 domain in β-spectrin (white) is bound to F-actin (purple) with Cys 112 located just outside the spectrin–actin contact. (*B*) β-spectrin repeats 14–15 constitute the ankyrin binding site (cyan side chains), and Cys 1883 is located on the same repeat but not within the ankryin binding site. (*C*) α-spectrin repeat 5, located adjacent to the tetramerization site, laterally associates with β-spectrin. Side chains of amino acids in contact are cyan. Cys 473 is on the opposite face of this interacting helix.

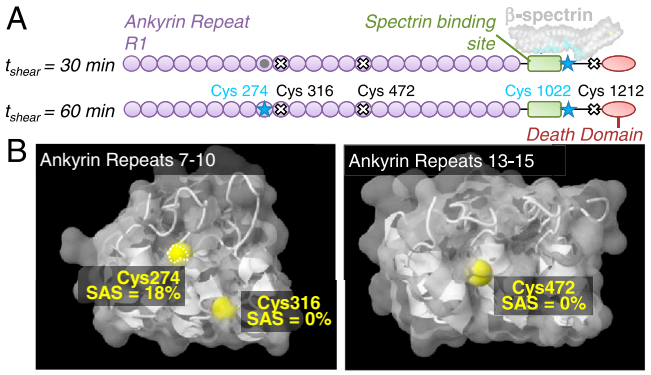

Fig. 7. Ankyrin Cys-labeling detected by mass spectrometry. Ankyrin repeat domains, structurally defined as two alpha helices separated by β-turns, are also reported to respond to mechanical stress, providing the molecular basis for overall protein flexibility. (*A*) The schematic respectively shows ankyrin repeats, the spectrin binding domain, and the death domain as purple circles, a green rectangle, and a red oval. Labeling of cysteines detected by mass spectrometry is represented in Fig. 5, where blue stars indicate force-enhanced labeling, gray circles represent force-independent labeling, and white x's indicate cysteines where only the modified peptide was detected. Force-enhanced labeling of Cys 1022 occurs at both 30 and 60 min of moderate shear (1.5 Pa). Cys 316 and Cys 472 are predicted to be buried, whereas Cys 274 is partially exposed to solution. (*B*) Homology models based on crystal structures for human Ankyrin R illustrate spatial relationships of detected Cys to known ankyrin binding interfaces. For both structures, the ankyrin groove faces out of the page.

Ankyrin Labeling Is Shear-Enhanced in Ankyrin Repeats and Near the Spectrin Binding Site. Sequence coverage of ankyrin ranged from 38% to 52%, with five detected cysteines spread along the protein (Fig. 7*A* and Table S4). Three detected Cys are in ankyrin repeats, two of which, Cys 316 and Cys 472, are predicted to be completely buried (Fig. 7*B*). Cys 274 in ankyrin repeat 8 shows force-enhanced labeling only at 60 min and contributes to the stress-enhanced labeling measured in densitometry of SDS-PAGE gels (Fig. 3*A*). (Φ)-values could not be calculated for Cys 316 and 472 in ankyrin repeats 9 and 14, respectively, or Cys 1212 because only peptides with fluorescently modified cysteines were detected, suggesting that these are highly reactive surface sites that are well-labeled under static conditions. Such sites would not contribute to stress-enhanced labeling. Ankyrin repeats 7–12, containing Cys 274 and 316, interact with one dimer of the band 3 tetramer, and repeats 13–24, containing Cys 472, interact with the other. The ankyrin groove surfaces directly associate with band 3 dimers (26). Cys 274 is located at the end of a helix, faces directly into the ankyrin groove, and is probably shielded by band 3 binding. Force-enhanced labeling could result from fluctuations in ankyrin–band 3 association after 60 min of shear. Cys 316 faces the interface of four repeat helices and is located on a helix in the outer row. The ankyrin superhelix is sufficiently elastic to stretch before unfolding occurs (27). Stress on the membrane propagating through band 3 could also stretch the ankyrin groove. Helices in the outer row are less tightly packed, increasing chances for solvent exposure of Cys 316 during shear. Cys 472 also faces the ankyrin groove but is not solvent accessible and does not likely participate directly in interactions with band 3. A high degree of labeling suggests that the ankyrin repeats experience a high degree of structural strain, even at short times.

Cys 1022 shows force-enhanced labeling at 30 and 60 min and is within only a dozen residues of the β-spectrin–ankyrin inter-

face. The extent and kinetics of stress-enhanced labeling of this site $\varphi_{30',60'} = (1.61,1.76)$ are similar to that of β-spectrin Cys 1883 $\varphi_{30',60'} = (1.52,1.68)$. The comparison suggests a similar mechanism of perturbation, which is detected only at high stress (Fig. 3*A*) and therefore suggests forced dissociation of spectrin–ankyrin, which increases Cys 1022 exposure to solvent.

Conclusions

Both spectrin unfolding and spectrin dissociation from the network appear to contribute to the RBC's response to mechanical stress. At low stress, repeat unfolding resulted in enhanced spectrin labeling that was equal for both antiparallel chains, whereas other cytoskeletal proteins were labeled independent of stress. Simultaneous enhanced labeling of spectin, actin, and ankyrin at high stress points to coordinated events, confirmed after examination of individual domain labeling with mass spectrometry. Fast labeling of Cys at high stress proximal to the spectrin–ankyrin junction verified the weaker ankyrin–spectrin affinity, as compared to the spectrin–actin-4.1R interaction. Stress-enhanced labeling of solution-exposed Cys in the region of spectrin–actin interaction signaled quaternary structure changes in the cytoskeletal network. Loss of coordinated, stress-enhanced labeling in the absence of 4.1R illustrates this protein's crucial role in maintaining network integrity, opposing spectrin–actin dissociation up to intermediate shear stress.

Mutant cells have the potential for abnormal molecular responses, and preliminary results on human RBCs with spectrin mutations that lead to an elliptocyte morphology and mechanical fragility similar to 4.1R deficiency (28) also indicate stress-accelerated spectrin labeling (Fig. S3). Although more study is needed to understand differences from normal cells, the shear-enhanced labeling at 60 min (1 Pa) appears similar to that of 4.1R-null cells here and below that of normal RBC (Fig. 2*C*). Nonetheless, the many complex mechanisms of molecular failure under stress motivate continued study of a type illustrated in Fig. S4 where we show (*i*) strong Cys labeling of membrane fragments generated at very high shear (4 Pa) consistent with rupture-enhanced labeling; (*ii*) treatment of ghosts with 1.5 M urea increases the amount of Cys labeling consistent with partial unfolding and/or dissociation; (*iii*) solubilized spectrin is labeled more than membrane-assembled spectrin, which seems consistent with Cys shielding by 4.1R, ankyrin, and/or actin in the membrane.

CS-MS reveals several types of structural changes, and labeling kinetics provide valuable insight into molecular processes within the network, with some tentative distinctions between weak and strong interactions. All of the spectrin Cys that were concluded here to be significantly stress-enhanced in labeling are in domains with melting temperatures $T_m > 37\,^{\circ}\mathrm{C}$ based on studies of individual domains (Fig. S5) (8) or purified intact protein (7). In other words, these domains should be mostly folded at the temperature used in these studies, but force is seen to unfold the domains in intact membranes. T_m's otherwise correlate poorly with the extent of force-enhanced Cys labeling, which illustrates the limited physiological insight obtained from traditional melting studies. Membrane curvature on a length scale of microns likewise shows no detectable correlation with labeling (Fig. S6): Indeed, labeling appears homogeneous on the membrane within approximately 10%. The present studies thus suggest a temperature threshold to the stress-dependent, homogeneous dynamics of protein interactions and domain folding. It is also now clear that the cytoskeleton responds in a graded fashion to force, with the nature of structural change depending on the magnitude and duration of stress.

Materials and Methods

Information about reagents, the preparation of ghosts, cysteine labeling under shear, SDS-PAGE analysis, mass spectrometry analysis, and structure predictions can be found in *SI Materials and Methods*.

ACKNOWLEDGMENTS. We thank Dr. Sara Saad (Universidade Estadual de Campinas, São Paulo, Brazil) for providing spectrin-mutant cells for initial study. We are grateful for support for this work from National Institutes of Health Grants R01HL062352 (to D.E.D.), P01DK032094 (to X.A., M.N., and D.E.D.), R01HL038794 (to D.W.S.), Interdisciplinary Cardiovascular T32 (C.C.K.), Penn's National Science Foundation–Nano Science Engineering Center (D.E.D. and C.C.K.), and the Human Frontiers Sciences Program (D.E.D.).

1. Mohandas N, Gallagher PG (2008) Red cell membrane: Past, present, and future. *Blood* 112:3939–3948.
2. Takakuwa Y, Tchernia G, Rossi M, Benabadji M, Mohandas N (1986) Restoration of normal membrane stability to unstable protein 4.1-deficient erythrocyte membranes by incorporation of purified protein 4.1. *J Clin Invest* 78:80–85.
3. Bennett V, Healy J (2009) Membrane domains based on ankyrin and spectrin associated with cell-cell interactions. *Cold Spring Harb Perspect Biol* 1:a003012.
4. Giorgi M, Cianci CD, Gallagher PG, Morrow JS (2001) Spectrin oligomerization is cooperatively coupled to membrane assembly: A linkage targeted by many hereditary hemolytic anemias. *Exp Mol Pathol* 70:215–230.
5. Johnson CP, Tang HY, Carag C, Speicher DW, Discher DE (2007) Forced unfolding of proteins within cells. *Science* 317:663–666.
6. Brandts JF, Erickson L, Lysko K, Schwartz AT, Taverna RD (1977) Calorimetric studies of the structural transitions of the human erythrocyte membrane. The involvement of spectrin in the A transition. *Biochemistry* 16:3450–3454.
7. An X, et al. (2006) Conformational stabilities of the structural repeats of erythroid spectrin and their functional implications. *J Biol Chem* 281:10527–10532.
8. Rief M, Pascual J, Saraste M, Gaub HE (1999) Single molecule force spectroscopy of spectrin repeats: Low unfolding forces in helix bundles. *J Mol Biol* 286:553–561.
9. Law R, et al. (2003) Cooperativity in forced unfolding of tandem spectrin repeats. *Biophys J* 84:533–544.
10. Ortiz V, Nielsen SO, Klein ML, Discher DE (2005) Unfolding a linker between helical repeats. *J Mol Biol* 349:638–647.
11. Johnson CP, et al. (2007) Pathogenic proline mutation in the linker between spectrin repeats: Disease caused by spectrin unfolding. *Blood* 109:3538–3543.
12. An X, Lecomte MC, Chasis JA, Mohandas N, Gratzer W (2002) Shear-response of the spectrin dimer-tetramer equilibrium in the red blood cell membrane. *J Biol Chem* 277:31796–31800.
13. Tchernia G, Mohandas N, Shohet SB (1981) Deficiency of skeletal membrane protein band 4.1 in homozygous hereditary elliptocytosis. Implications for erythrocyte membrane stability. *J Clin Invest* 68:454–460.
14. Chiancone E, Currell DL, Vecchini P, Antonini E, Wyman J (1970) Kinetics of the reaction of the "masked" and "free" sulfhydryl groups of human hemoglobin with p-mercuribenzoate. *J Biol Chem* 245:4105–4111.
15. Ohanian V, et al. (1984) Analysis of the ternary interaction of the red cell membrane skeletal proteins spectrin, actin, and 4.1. *Biochemistry* 23:4416–4420.
16. Discher DE, et al. (1995) Mechanochemistry of protein 4.1's spectrin-actin binding domain: Ternary complex interactions, membrane binding, network integration, structural strengthening. *J Cell Biol* 130:897–907.
17. Salomao M, et al. (2008) Protein 4.1R-dependent multiprotein complex: New insights into the structural organization of the red blood cell membrane. *Proc Natl Acad Sci USA* 105:8026–8031.
18. Zhang D, Kiyatkin A, Bolin JT, Low PS (2000) Crystallographic structure and functional interpretation of the cytoplasmic domain of erythrocyte membrane band 3. *Blood* 96:2925–2933.
19. Discher DE, Boal DH, Boey SK (1998) Simulations of the erythrocyte cytoskeleton at large deformation. II. Micropipette aspiration. *Biophys J* 75:1584–1597.
20. Parry DA, Dixon TW, Cohen C (1992) Analysis of the three-alpha-helix motif in the spectrin superfamily of proteins. *Biophys J* 61:858–867.
21. Podgorski A, Alster P, Elbaum D (1988) Interactions among red cell membrane proteins. *Biochemistry* 27:609–614.
22. Kusunoki H, MacDonald RI, Mondragón A (2004) Structural insights into the stability and flexibility of unusual erythroid spectrin repeats. *Structure* 12:645–656.
23. Ipsaro JJ, Mondragón A (2010) Structural basis for spectrin recognition by ankyrin. *Blood* 115:4093–4101.
24. Stabach PR, et al. (2009) The structure of the ankyrin-binding site of β-spectrin reveals how tandem spectrin-repeats generate unique ligand-binding properties. *Blood* 113:5377–5384.
25. Li D, et al. (2010) A comprehensive model of the spectrin divalent tetramer binding region deduced using homology modeling and chemical cross-linking of a mini-spectrin. *J Biol Chem* 285:29535–29545.
26. Michaely P, Tomchick DR, Machius M, Anderson RG (2002) Crystal structure of a 12 ANK repeat stack from human ankyrinR. *EMBO J* 21:6387–6396.
27. Lee G, et al. (2006) Nanospring behaviour of ankyrin repeats. *Nature* 440:246–249.
28. Gallagher PG (2004) Hereditary elliptocytosis: spectrin and protein 4.1R. *Semin Hematol* 41:142–164.

Supporting Information

Krieger et al. 10.1073/pnas.1018887108

SI Materials and Methods.

Reagents. N-(4,4-difluoro-1,3,5,7-tetramethyl-4-bora-3a,4a-diaza-s-indacene-2-yl) iodoacetamide (BODIPY) and monobromobimane FluoroPure grade (mBBr) were purchased from Invitrogen. N-(Iodoacetaminoethyl)-1-naphthylamine-5-sulfonic acid (IAEDANS) and iodoacetamide (IAM) were purchased from Sigma.

Preparation of Ghosts. Fresh whole blood from 4.1R-null mice was shipped from the New York Blood Center together with WT blood, which was also sometimes purchased from Covance. Erythrocytes were segregated from whole blood by centrifugation and washed once with isotonic phosphate-buffered saline (PBS; 10 mM sodium phosphate, 150 mM potassium chloride, pH 7.4). Cells were then lysed in approximately 30 volumes hypotonic buffer (5 mM sodium phosphate, 5 mM potassium chloride, 2 mM magnesium chloride pH 7.4). White ghosts were washed with hypotonic buffer until hemoglobin was almost completely removed (approximately 5×) and resealed with isotonic buffer containing 200 μM IAEDANS (Sigma). Pink ghosts were not washed and were instead resealed immediately after lysis. Because the hemoglobin in pink ghosts would compete with spectrin for thiol label, pink ghosts were resealed in isotonic buffer containing 400 μM IAEDANS. The concentration of IAEDANS in pink ghosts was chosen so that the fluorescence intensity of spectrin matched the fluorescent intensity of spectrin in white ghosts loaded with 200 μM IAEDANS after static labeling. Both white and pink ghosts were resealed at room temperature for 30 min in the dark.

Labeling of Ghosts During Shear. Resealed ghosts were washed once in PBS, then resuspended in labeling solution containing 2 mM BODIPY 504/507 (Invitrogen) or for MS samples, mBBr (Invitrogen) in PBS. The suspension was divided into two samples. The static sample was covered in foil and incubated on a heat block at 37 °C, and the shear sample was loaded onto a temperature-controlled cone and plate rheometer set to 37 °C. Samples were then sheared at various stresses for up to 1 h, then washed once in ice-cold PBS. For kinetic mass spectrometry studies, ghosts were sheared for two time intervals, 30 and 60 min, where $t = 0$ designates the addition of the second dye. Previous Cys-labeling studies of RBC (1) have shown that 30 min of static labeling with IAEDANS is sufficient to saturate a large fraction of exposed Cys, establishing a baseline or background labeling. Additional shear labeling times were long enough to enhance the labeling above this background level.

SDS-PAGE Analysis. Ghosts prelabeled with IAEDANS, then labeled with BODIPY during shear were lysed with Radio-Immunoprecipitation Assay buffer containing 1% Triton-X 100 at 4 °C for 30 min, and lysates separated on 3–8% or 7% Tris-Acetate buffered polyacrylamide gels. Fluorescent images were taken immediately after the run was complete, and gels were stained with Coomasie R-250. Fluorescent and Coomassie intensities were measured using ImageJ. For wild-type red cells, lysates were run in multiple lanes with different loadings. Proteins were identified based on molecular weight. Fluorescent intensity versus Coomassie intensity plots were made for each band. If $R^2 < 0.9$, lysates were rerun on PAGE gels or experiments repeated. For most samples, $R^2 > 0.95$. Shear-enhanced labeling was calculated by the ratio of slopes of the sheared and static samples, with ratios > 1.1 considered shear-enhanced. All experiments with white ghosts were repeated at least twice, and error bars indicate the range of m_{shear}/m_{static} values at that shear stress. Experiments with pink ghosts were done once. Because of the scarcity of 4.1R-null sample, lystates were run in single lanes. Error bars are the estimated range of values based on the variation of 4.1R-null m_{static} values from three independent experiments. Fluorescent intensity was normalized by Coomassie intensity, and shear-enhanced labeling was calculated from the ratio of normalized shear : static fluorescent intensities.

Liquid Chromatography–Tandem Mass Spectrometry (LC-MS/MS) Analysis. For mass spectrometry analysis, ghosts were prelabeled with IAEDANS and then labeled with mBBr during shear. Lysates were made and separated as described above. Alpha and beta spectrin bands were excised for in-gel trypsin digest. Tryptic peptides were analyzed by LC-MS/MS on a LTQ-Orbitrap XL mass spectrometer (Thermo Fisher Scientific) interfaced with an Eksigent Autosampler/NanoLC-2D system (Eksigent Technologies). Peptides were eluted at 300 nL/min using an acetonitrile gradient consisting of 3–28% B over 40 min, 28–50% B over 25.5 min, 50–80% B over 5 min, 80% B for 5 min before returning to 3% B in 1 min. To minimize carryover, a blank cycle was run between each sample. The mass spectrometer was set to perform a full MS scan (m/z 350–2,000) in the Orbitrap, and the six most intense ions exceeding a minimum threshold of 1,000 were selected for MS/MS in the linear trap with dynamic exclusion enabled. Protein identification was done using the SEQUEST algorithm in BioWorks 3.3.1 (Thermo Fisher Scientific). Data were searched against a mouse database using a partial tryptic constraint with a 1.1 Da precursor mass tolerance, and allowing for methionine sulfoxide, IAM, IAEDANS, or mBBr cysteine modifications. Peptide identifications were filtered using the following criteria: mass tolerance ≤5 ppm, $\Delta Cn \geq 0.069$, and $Sf \geq 0.2$. The extent of IAEDANS, mBBr, and IAM labeling at each site was determined from extracted ion chromatograms with identification of each specific Cys achieved through both the m/z of the modified-Cys peptide as well as the MS/MS fragmentation pattern. Ion-flux values of Cys-labeled peptides from shear and static samples were normalized by their corresponding Cys-IAM ion-flux values. Phi values were calculated from the ratios of normalized shear and static ion fluxes, with phi > 1.25 defined as force-enhanced labeling. When multiple peptides were detected for the same cysteine, peptides with the greater ion-flux values were chosen to be represented in Fig. 5.

Sequence Alignment and Structure Predictions. Amino acids of alpha and beta spectrin were numbered according to UnitProt files P08032 and P15508, respectively. All alignments were done with ClustalW 2.0.12 (2). Solvent exposure of cysteines within repeat domains was estimated according to Parry et al. (3). Heptad position predicted was based on alignment with repeats 16–17 of chick nonerythrocytic spectrin, Protein Data Bank (PDB) ID code 1CUN. For Cys-β1159 position was based on alignment with repeats 8–9 in human erythrocytic spectrin, PDB ID code 1S35. For Cys-α129, the CH1 domain was aligned with human α-actinin 3, PDB ID code 3LUE. Cys-β1883 was aligned with repeats 14–15 of human spectrin, PDB ID code 3E57. Homology models for ankyrin cysteines Cys-274, Cys-316, and Cys-472 were aligned with the crystal structure of human ankyrinR repeat domains 13–24, PDB ID code 1N11. All homology models were generated by MODELLER 9v8 (4) based on ClustalW alignments. The coordinates of the mouse spectrin CH1 domain in reference to actin were determined using Chimera, based on the superposition of the homology model with the CH1 domain in PDB ID code

3LUE. All images of homology models were produced using Jmol.

Fluorescent Labeling of Fragments. Wild-type ghosts were loaded with BODIPY as described above, then incubated at 37 °C under 4 Pa shear stress or static conditions. Postthiol labeling, DiI, and glutathione (final concentration 10 mM) were added to the reaction solution and incubated for 20 min at room temperature to label membrane and quench excess dye.

Antibodies and Immunostaining. Anti-mouse CD47 antibodies were obtained from BD Biosciences (clone miap301). Secondary antibody used to detect CD47 was goat anti-rat IgG R-phycoerythrin purchased from Invitrogen. Post BODIPY labeling at 37 °C during 1.5 Pa shear and static conditions were incubated with CD47 antibody in PBS (1:500) for 20 min at room temperature. Ghosts were washed and incubated with secondary in PBS (1:1000) with DiI for 20 min at room temperature followed by washing and imaging on polylysine coated coverslips.

Fluorescent Imaging of Ghosts. For quantitative microscopy, ghosts were prelabeled with IAEDANS, then incubated with BODIPY and labeled under 1 or 2 Pa shear stress or static conditions. Fluorescent images of labeled ghosts were taken on an inverted microscope (IX71; Olympus) with a 60× (oil, 1.4 NA) objective using a Cascade CCD camera (Photometrics). Background subtraction and subsequent image analysis was done using ImageJ. Image acquisition was performed with Image Pro software (Media Cybernetics, Inc.) and results are shown in Fig 2*C*. Representative images from these experiments are displayed in Fig 1*C* as "0 Pa," "1 Pa," and "2 Pa." Ghosts BODIPY labeled during 1.5 Pa shear stress and immunostained for CD47 were imaged using a 150× (oil, 1.45 NA) objective. A side-view static-labeled ghost from this experiment appears in Fig S4*B*. Fragments were also imaged using the 150× objective.

1. Johnson CP, Tang HY, Carag C, Speicher DW, Discher DE (2007) Forced unfolding of proteins within cells. *Science* 317:663–666.
2. Thompson JD, Higgins DG, Gibson TJ (1994) CLUSTAL W: Improving the sensitivity of progressive multiple sequence alignment through sequence weighting, position-specific gap penalties and weight matrix choice. *Nucleic Acids Res* 22:4673–4680.
3. Parry DA, Dixon TW, Cohen C (1992) Analysis of the three-alpha-helix motif in the spectrin superfamily of proteins. *Biophys J* 61:858–867.
4. Sali A, Blundell TL (1993) Comparative protein modelling by satisfaction of spatial restraints. *J Mol Biol* 234:779–815.

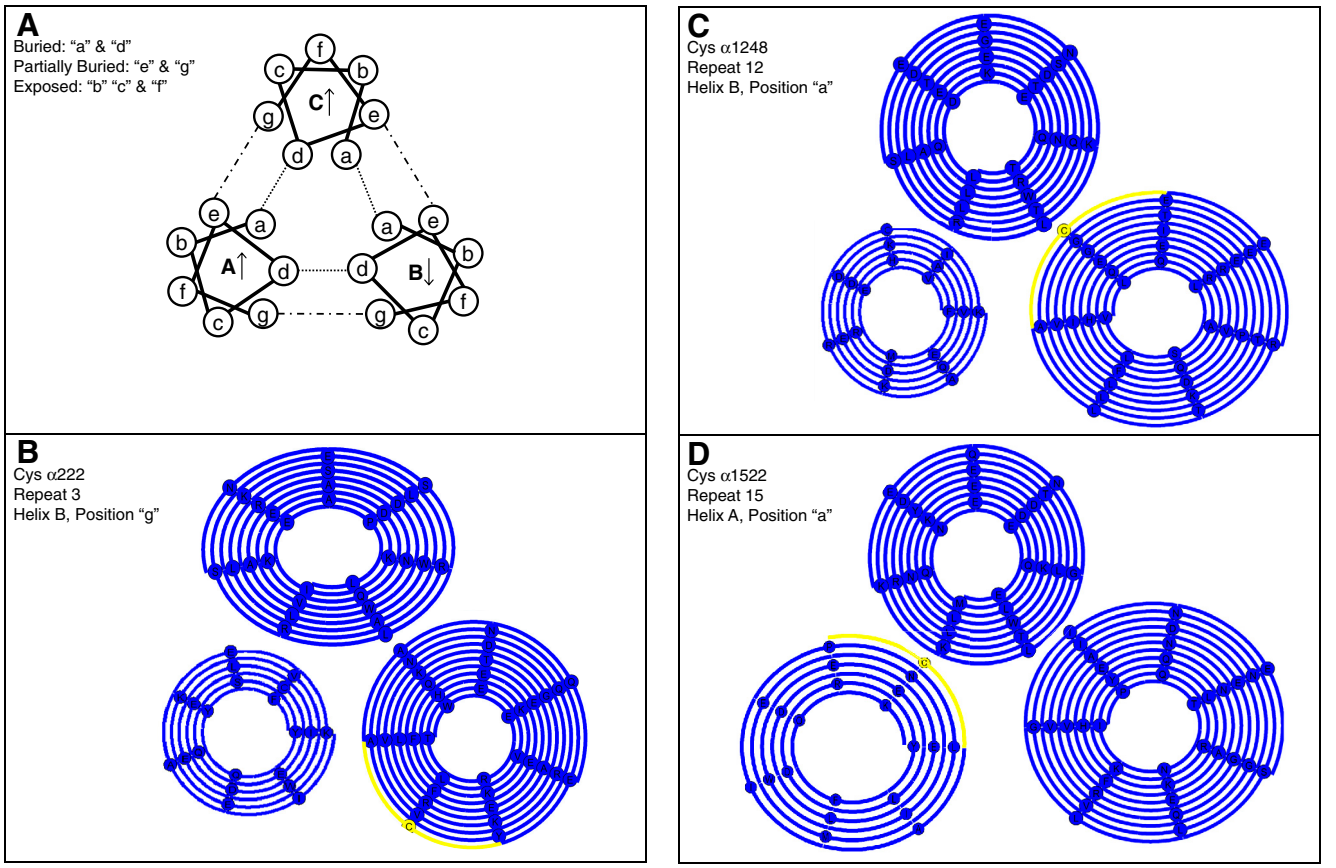

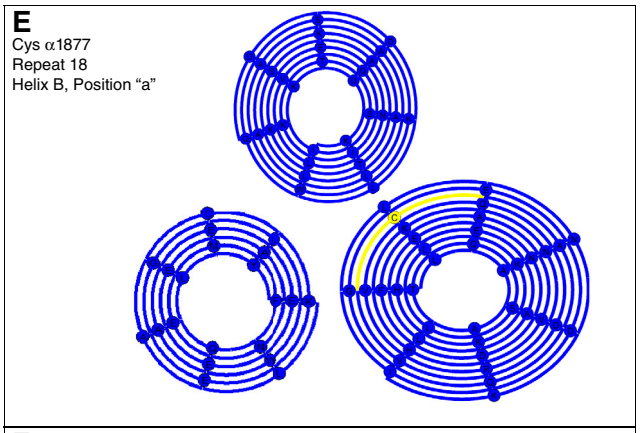
E
Cys α1877
Repeat 18
Helix B, Position "a"

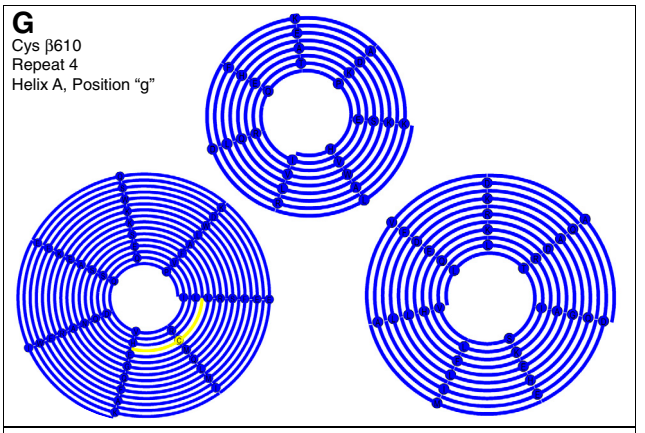
G
Cys β610
Repeat 4
Helix A, Position "g"

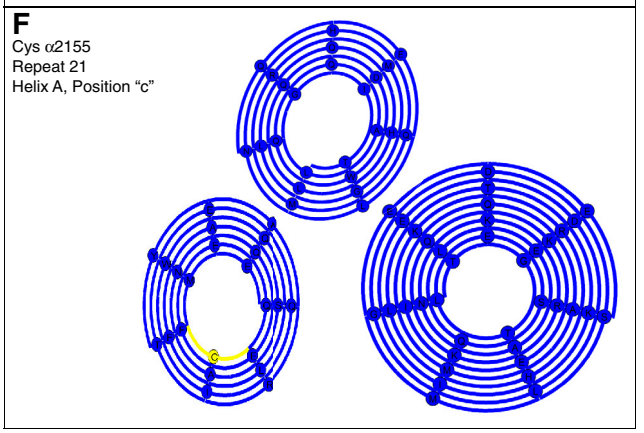
F
Cys α2155
Repeat 21
Helix A, Position "c"

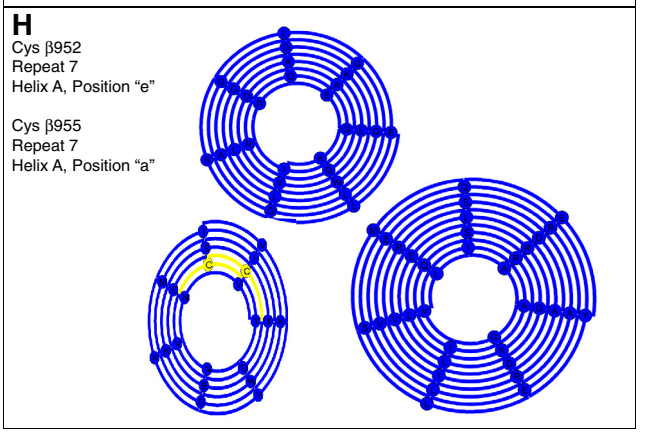
H
Cys β952
Repeat 7
Helix A, Position "e"
Cys β955
Repeat 7
Helix A, Position "a"

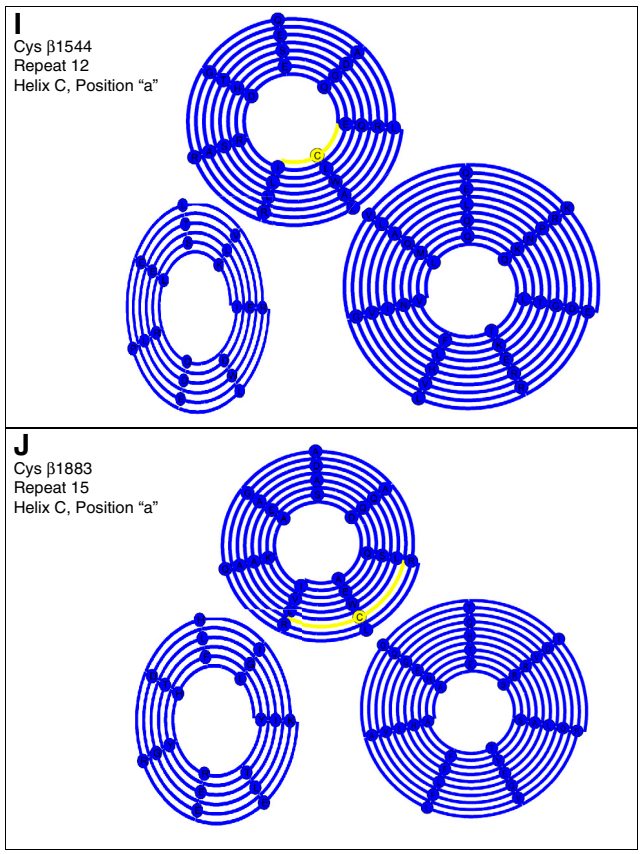

Fig. S1. Helical wheel depictions of repeat domains indicating hydrophobically shielded cysteines. Repeat domains containing detected cysteines were represented as helical wheels. (*A*) Helices are viewed from the N terminus and show left-handed connectivity. Helices A, B, and C are the first, second, and third helix of the repeat domain, respectively. Arrows point from the N-terminal end to the C-terminal end of the helix. Heptad positions are labeled "a" to "g." Positions "a" and "d" are considered shielded from the aqueous environment. Positions "e" and "g" often participate in interhelix associations are defined as partially buried (2). Amino acids in linkers connecting helices are not shown. (*B–J*) Helical wheels of repeat domains. Heptad assignment was made according to sequence alignment with PDB ID codes 1CUN, 1S35, or 3E57 (*SI Materials and Methods*). Detected cysteines are colored yellow.

Fig. S2. Spectrin mouse and human sequence alignments. Domain sequences in mouse spectrin were aligned to sequences of existing crystal structures (see *SI Materials and Methods*), and the alignments shown to compare the location of detected cysteines to other functionally important amino acids or previously detected cysteines. In all alignments, detected cysteines are highlighted in yellow. Below each sequence, identical, conserved, and semiconserved amino acids are indicated by asterisks, colons, and periods, respectively. (*A*) The cysteine in the helical linker between β-spectrin repeats 8–9 has been previously detected (1). In this alignment, the helices of repeats 8 and 9 have been highlighted in cyan and light green, respectively, with the positions of "a" and "d" amino acids labeled above. The helical linker connecting repeats are shown in magenta, and the mouse and human forms differ by one amino acid. (*B*) The actin binding domain of mouse spectrin was aligned to that of human alpha-actinin1 to compare the location of Cys β112 of amino acids known to interact with actin. The helices of the CH1 and CH2 domains are highlighted in red and cyan, respectively, with their a–g identity labeled above. Amino acids in light green are surface exposed and believed to directly participate in the interaction with actin. The detected cysteine is within helix "e" of CH1, and its position on the helix shows that it is not of the same face as surface exposed amino acids and is probably not within the spectrin–actin interface. (*C*) Mouse and human β-spectrin repeats 13–15 were aligned to compare the location of Cys β1883 to ankyrin binding amino acids (cyan). The helices of repeats 13, 14, and 15 are highlighted in light green, red, and teal, respectively. The helical linker between repeats 13 and 14 is highlighted in light gray. The helical linker represents a stuttering in the a–g heptad ordering that occurs between repeats 13 and 14. According to the crystal structures for human repeats 14–15, such a stuttering does not occur between those repeats. The detected cysteine was distally located from ankyrin binding amino acids; however, it is possible that structural perturbations distal from the ankyrin binding site can affect spectrin–ankyrin interaction, as demonstrated by the locations of mutation sites previously found to destabilize spectrin–ankyrin binding (magenta).

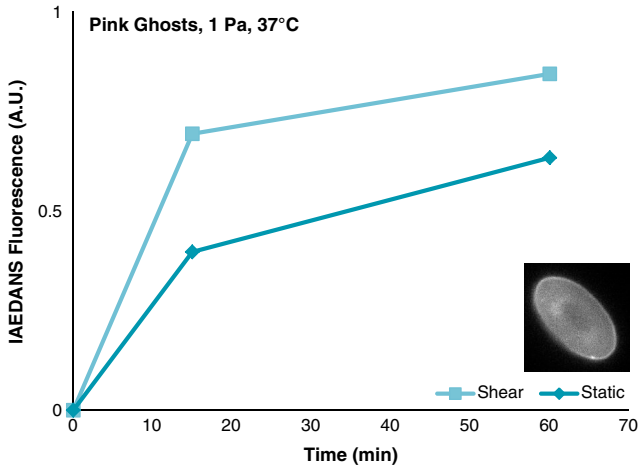

Fig. S3. Accelerated Cys labeling of spectrin in Wagner erythrocytes. Human Wagner erythrocytes containing spectrin with a currently uncharacterized mutation were generously provided by the Saad group (State University of Campinas). IAEDANS-labeled Wagner ghost reveals elliptocyte morphology characteristic of spectrin mutations. After normalizing IAEDANS fluorescence by Coomassie intensity, $\Phi_{15'} \approx 1.7$ and $\Phi_{60'} \approx 1.3$. The latter is closer to the result determined for 4.1R null cells in Fig. 2*C*.

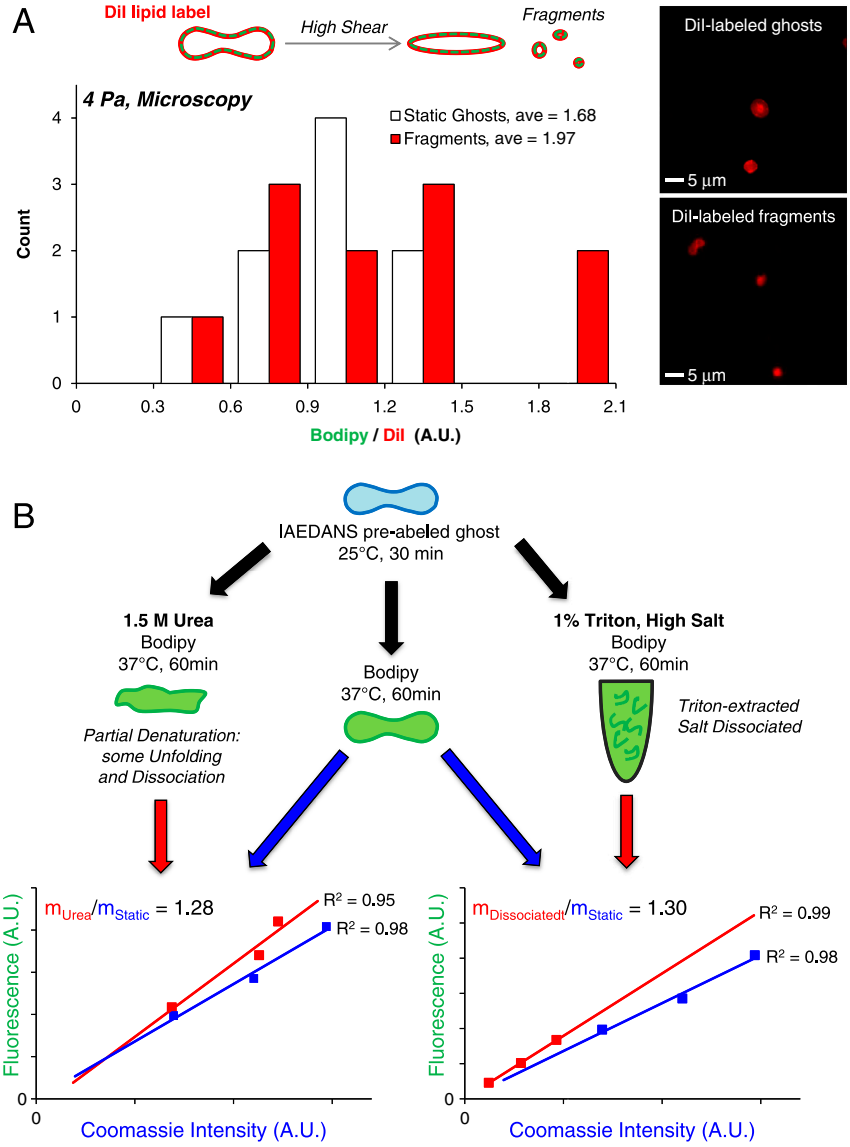

Fig. S4. Spectrin dissociation from binding partners increases cysteine labeling. Although network rupture ultimately removes stress on spectrin, immediately before rupture occurs, the spectrin network is extremely stressed, resulting in an increase in cysteine labeling. To show this, BODIPY labeling of fragments from stress-ruptured ghosts was compared to labeling of intact static-labeled ghosts (*Materials and Methods*). (*A*) Shearing at 4 Pa for 60 min creates fragments detectable by DiI. A histogram of BODIPY/DiI ratios, normalized to average BODIPY/DiI for static ghosts, shows increase variation of values for fragments. Although analysis is complicated by loss of spectrin in fragments, average BODIPY fluorescence, normalized by DiI intensity, approximately 17% greater for fragments than for whole ghosts. (*B*) After rupture, decrease in stress-induced unfolding is accompanied by exposure of cysteines ordinarily shielded by quaternary association. Ghosts were static labeled with BODIPY in PBS, 1.5 M urea, and 300 mM NaCl (*Materials and Methods*) to assess spectrin labeling in a network, under denatured conditions, and in a solubilized form. As previously shown (1), urea denaturation increases cysteine labeling. Under Triton-extracted, high salt conditions, spectrin is completely solubilized. Cysteines hydrophobically buried in repeat domains are shielded from solution while cysteines in binding sites are exposed to thiol probe, resulting in 30% greater labeling.

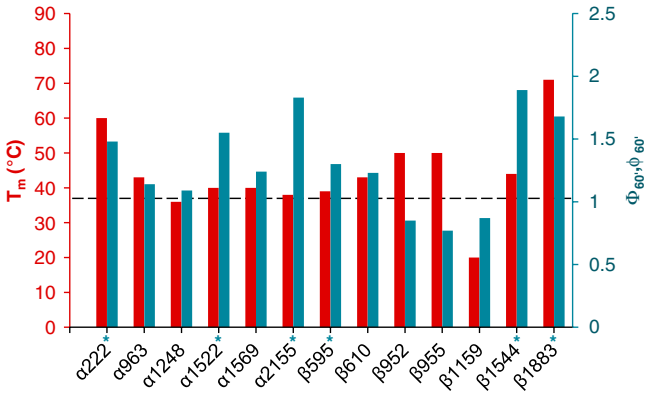

Fig. S5. T_M of human spectrin repeat domains compared with mouse spectrin $\Phi_{60'}$, $\varphi_{60'}$ Melting temperatures of individual repeat domains (1) were compared to $\Phi_{60'}$, $\varphi_{60'}$ values shown in Table S1. Blue asterisks correspond to blue stars in Fig. 5.

1. An X, Lecomte MC, Chasis JA, Mohandas N, Gratzer W (2002) Shear-response of the spectrin dimer-tetramer equilibrium in the red blood cell membrane. *J Biol Chem* 277:31796–31800.

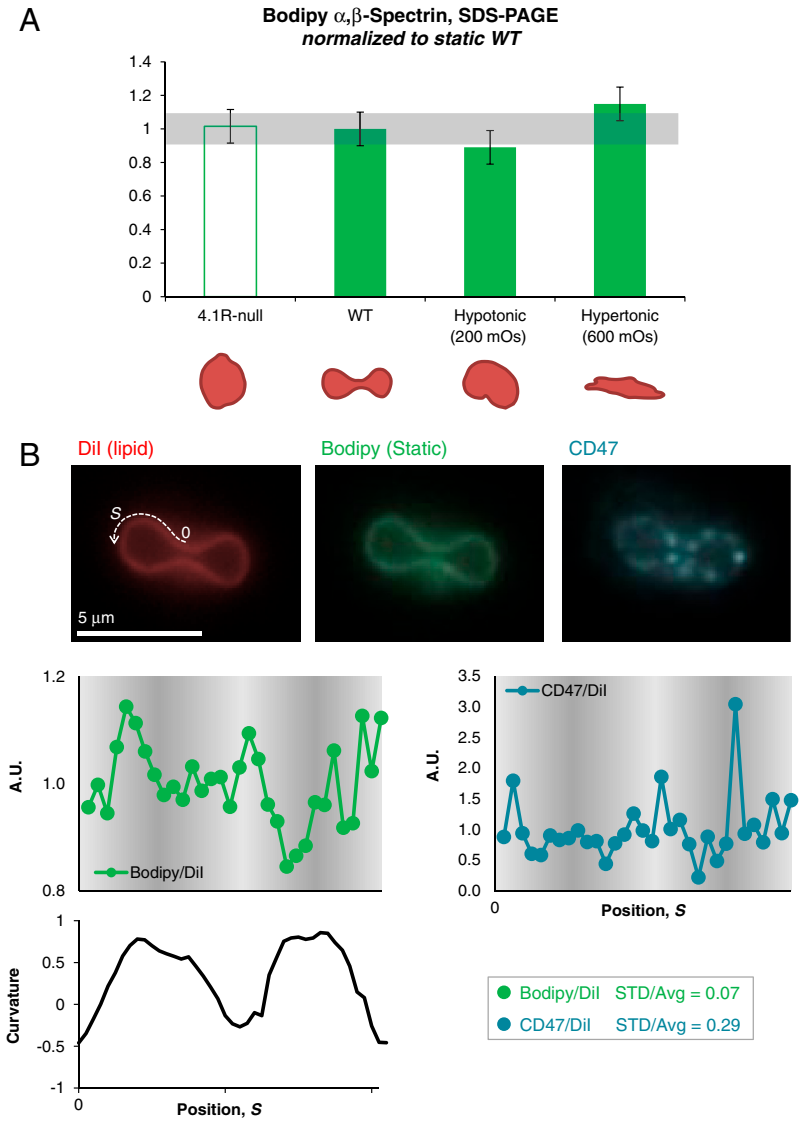

Fig. S6. Curvature effects on cysteine labeling. (*A*) 4.1R-null and wild-type RBC were static-labeled with two dyes under isotonic, hypotonic, and hypertonic buffers demonstrate the effects of curvature on spectrin labeling. IAEDANS prelabeled ghosts (blue) were split and incubated with BODIPY dye (green) under different osmotic conditions then subjected to SDS-PAGE analysis for spectrin (*Materials and Methods*). Ghosts in hypotonic buffer have less curvature and more closely resemble 4.1R-null ghosts in isotonic buffer, whereas ghosts in hypertonic buffer are flatter with some regions of high curvature, and yet spectrin labeling is not significantly different (within 10%). (*B*) BODIPY labeling along the membrane, normalized by DiI fluorescence in a side view of a ghost statically labeled in isotonic buffer shows that there is little variation in BODIPY labeling and again little correlation with membrane curvature. This is in contrast to CD47, which shows a high degree of variation along the membrane (note scale of graph and mean deviation) as we reported previously (1).

1. Subramanian et al. (2006) Membrane mobility and clustering of Integrin Associated Protein (IAP, CD47)—major differences between mouse and man and implications for signaling. *Blood Cell Mol Dis* 36:364–372.

Table S1. Rate constants from force-dependent Linderstrom–Lang fits of wild-type and 4.1R-null ghosts

Sample	$k_{1f}(\text{min}^{-1})$	$k_{1r}(\text{min}^{-1})$	R^2
WT, white ghosts	0.04	0.27	0.98
4.1-null, white ghosts	0.02	0	0.76

SDS-PAGE data was fit for k_{1f} and k_{1r} using the force-dependent Linderstrom–Lang equation previously described (1). Values for Δx and $\Delta x'$ were derived from previous single molecule experiments on spectrin repeats and have not changed from our earlier Cys labeling of human RBC. Shear area was reduced in proportion to the decrease in mouse to human red cell surface area. Parameter $k_2[\text{dye}] = 0.13\ \text{min}^{-1}$ as was determined from these earlier studies and held constant for wild-type and 4.1-null fits. Note that the zero time point in Fig. 2*C* reflects real data with error. The mechanical fragility was hypothesized to be due to a weakened spectrin–actin interaction, which is also reflected in the lower unfolding rate for 4.1R-null spectrin. If this dissociation occurs, cysteines in 4.1R null spectrin are not exposed due to force-induced unfolding but rather thermal fluctuations. For pink ghosts, $k_2[\text{dye}]$ was decreased to $0.085\ \text{min}^{-1}$, assuming k_{1f} and k_{1r} do not change from wild-type white ghosts parameters. Given the higher concentration of hemoglobin in pink compared to white ghosts, a lower effective labeling rate is expected.

Table S2. Cys-labeling ratios for spectrin peptides quantified by mass spectrometry

				IAEDANS		mBBr	
Peptide	Cys	Domain	Predicted accessibility	$\Phi_{30'}$	$\Phi_{60'}$	$\varphi_{30'}$	$\varphi_{60'}$
FYQYSQECEDILEWVK	α165	ABD	—			0.93	0.80
VNQYANECAQEK	α222	R3	partially buried	1.04	1.50	0.86	1.48
QCLDFHLFYR	α473	linker	—	1.43	1.60		
DQAEVCQQQQAAPVDEAGR	α963	R10	—			0.88	1.14
LCESHPDATEDLQK	α1248	R12	buried			0.88	1.09
DLEDLEEWINEMLPIACDESYK (4–5%)	α1522	R15	buried			1.32	2.43
DLEDLEEWINEMLPIACDESYKDPTNIQR						1.16	1.55
VCDGDEENMQEQLDK	α1569	R15B,Clinker	exposed	1.26	1.26	1.02	1.24
RVCDGDEENMQEQLDK (5–37%)				1.04	1.69	0.96	1.88
VQDVCAQGEDILNK	α1877	R18	buried			0.98	1.34
VQDVCAQGEDILNKEETQNK (30–41%)						1.17	1.45
NFEMCQEFEQNASAFLQWIQETR	α2155	R21	exposed	2.12	3.88	1.13	1.83
IHCLENVDK	β112	CH 1	—	0.76	1.83		
GYQPCDPQVIQDR	β595	R3B,Clinker	exposed	0.90	1.56	0.80	1.30
VSHLEQCFSELSNMAAGR	β610	R4	partially buried	1.22	1.67	1.02	1.23
VNNYCVDCEETSK	β952	R7	partially buried	0.76	1.23	0.84	0.85
$VNNYC_{mbbr}VDC_{mbbr}EETSK$	β955	R7	buried			0.57	0.77
$VNNYC_{IAEDANS}VDC_{mbbr}EETSK$						0.57	0.87
GNTLTQCLGFQEFQK	β1159	linker	—			0.99	0.87
AAEIDCQDIEER	β1544	R12	buried	0.90	1.46	0.81	1.89
EQEVSAAWQALLDACAGR	β1883	R15	buried	1.86	2.13	1.52	1.68

WT ghosts were prelabeled with IAEDANS under static conditions at room temperature for 30 min and then labeled with both IAEDANS and mBBr under shear conditions for 30 or 60 min. The Cys peptides detected by MS are listed together with amino acid number, spectrin domain, and predicted accessibility within the domain. Φ_{time} and φ_{time} are the ion-flux ratios of IAEDANS/IAM and mBBr/IAM Cys peptides, respectively, and are a measure of the force-enhanced labeling for individual cysteines (see Table S3 for raw data). Φ_{time} or φ_{time} values in bold indicate ion-flux ratios ≥ 1.25, which we define as force-enhanced labeling in Fig. 4. In cases of multiple peptides or labeling states, peptides with the greater ion flux were given preference (see Table S3). Cys β955 presents a special case, where the close proximity of Cys β952 and β955 results in multiple labeled states for a single peptide. The φ_{time} values for $VNNYC_{mbbr}VDC_{mbbr}EETSK$ are the ratios of the double mBBr labeled peptide to the completely unmodified peptide. $VNNYC_{IAEDANS}VDC_{mbbr}EETSK$ φ_{time} values represent the ratios of that peptide to the completely unmodified peptide. This peptide in the double IAEDANS labeled form was not detected. Nor were peptides with only Cys β955 modifiations. In this study these cysteines were classified as force-independently labeled, and further kinetic mass spectrometry studies are needed to clarify this complex behavior

Table S3. Ion-flux data of mass-spectometry detected peptides, α,β-spectrin

Peptide	Cys	$ST_{30'}$	$SH_{30'}$	$ST_{60'}$	$SH_{60'}$
FYQYSQEC$_{[IAM]}$EDILEWVK	α165	1.07E + 09	8.42E + 08	1.28E + 09	8.17E + 08
FYQYSQEC$_{[IAEDANS]}$EDILEWVK		2.81E + 07	2.06E + 07	4.05E + 07	2.06E + 07
VNQYANEC$_{[IAM]}$AQEK	α222	5.24E + 08	5.47E + 08	7.83E + 08	4.84E + 08
VNQYANEC$_{[IAEDANS]}$AQEK		1.14E + 07	1.24E + 07	1.60E + 07	1.48E + 07
VNQYANEC$_{[mBBr]}$AQEK		6.71E + 08	6.02E + 08	6.86E + 08	6.27E + 08
QC$_{[IAM]}$LDFHLFYR	α473	9.62E + 06	8.32E + 06	1.83E + 07	1.10E + 07
QC$_{[IAEDANS]}$LDFHLFYR		2.71E + 07	3.35E + 07	3.44E + 07	3.30E + 07
DQAEVC$_{[IAM]}$QQQQAAPVDEAGR	α963	3.69E + 08	3.63E + 08	5.15E + 08	3.53E + 08
DQAEVC$_{[mBBr]}$QQQQAAPVDEAGR		1.87E + 09	1.61E + 09	2.26E + 09	1.77E + 09
LC$_{[IAM]}$ESHPDATEDLQK	α1248	2.72E + 08	2.70E + 08	3.51E + 08	2.71E + 08
LC$_{[IAEDANS]}$ESHPDATEDLQK		9.71E + 08	8.75E + 08	1.33E + 09	1.05E + 09
LC$_{[mBBr]}$ESHPDATEDLQK		6.19E + 08	5.42E + 08	7.52E + 08	6.30E + 08
DLEDLEEWINEMLPIAC$_{[IAM]}$DESYK (4%)	α1522	1.78E + 07	1.58E + 07	1.99E + 07	1.82E + 07
DLEDLEEWINEMLPIAC$_{[mBBr]}$DESYK (3–5%)		1.86E + 07	2.38E + 07	1.14E + 07	2.34E + 07
DLEDLEEWINEMLPIAC$_{[IAM]}$DESYKDPTNIQR		3.81E + 08	3.69E + 08	5.00E + 08	4.22E + 08
DLEDLEEWINEMLPIAC$_{[mBBr]}$DESYKDPTNIQR		3.99E + 08	4.48E + 08	3.20E + 08	4.21E + 08
VC$_{[IAM]}$DGDEENMQEQLDK	α1569	8.74E + 07	6.74E + 07	1.12E + 08	7.62E + 07
VC$_{[IAEDANS]}$DGDEENMQEQLDK		1.04E + 08	1.01E + 08	1.62E + 08	1.39E + 08
VC$_{[mBBr]}$DGDEENMQEQLDK		1.29E + 09	1.02E + 09	1.54E + 09	1.30E + 09
RVC$_{[IAM]}$DGDEENMQEQLDK (20–27%)		2.14E + 07	2.26E + 07	4.04E + 07	1.92E + 07
RVC$_{[IAEDANS]}$DGDEENMQEQLDK (32–37%)		5.42E + 07	5.93E + 07	8.23E + 07	6.56E + 07
RVC$_{[mBBr]}$DGDEENMQEQLDK (5–6%)		6.45E + 07	6.53E + 07	8.00E + 07	7.14E + 07
VQDVC$_{[IAM]}$AQGEDILNK	α1877	1.83E + 09	1.45E + 09	2.58E + 09	1.50E + 09
VQDVC$_{[mBBr]}$AQGEDILNK		1.62E + 08	1.26E + 08	1.59E + 08	1.24E + 08
VQDVC$_{[IAM]}$AQGEDILNKEETQNK (30–34%)		7.81E + 08	7.38E + 08	1.13E + 09	6.70E + 08
VQDVC$_{[mBBr]}$AQGEDILNKEETQNK (38–41%)		1.01E + 08	1.11E + 08	1.00E + 08	8.60E + 07
NFEMC$_{[IAM]}$QEFEQNASAFLQWIQETR	α2155	2.53E + 07	2.33E + 07	3.72E + 07	3.07E + 07
NFEMC$_{[IAEDANS]}$QEFEQNASAFLQWIQETR		2.05E + 06	3.99E + 06	9.85E + 05	3.16E + 06
NFEMC$_{[mBBr]}$QEFEQNASAFLQWIQETR		3.80E + 08	3.94E + 08	2.92E + 08	4.41E + 08
IHC$_{[IAM]}$LENVDK	β112	1.19E + 08	9.31E + 07	2.64E + 08	1.77E + 08
IHC$_{[IAEDANS]}$LENVDK		3.58E + 08	2.13E + 08	3.27E + 08	4.00E + 08
GYQPC$_{[IAM]}$DPQVIQDR	β595	8.09E + 07	5.56E + 07	1.47E + 08	1.05E + 08
GYQPC$_{[IAEDANS]}$DPQVIQDR		2.20E + 08	1.36E + 08	2.00E + 08	2.28E + 08
GYQPC$_{[mbbr]}$DPQVIQDR		1.98E + 09	1.09E + 09	2.37E + 09	2.14E + 09
VSHLEQC$_{[IAM]}$FSELSNMAAGR	β610	3.68E + 08	2.32E + 08	6.38E + 08	4.84E + 08
VSHLEQC$_{[IAEDANS]}$FSELSNMAAGR		2.84E + 07	2.19E + 07	2.52E + 07	3.19E + 07
VSHLEQC$_{[mbbr]}$FSELSNMAAGR		1.11E + 09	7.16E + 08	1.30E + 09	1.25E + 09
VNNYC$_{[IAM]}$VDC$_{[IAM]}$EETSK (5–6%)	β952	1.79E + 07	1.32E + 07	3.79E + 07	2.96E + 07
VNNYC$_{[IAEDANS]}$VDC$_{[IAM]}$EETSK (11–15%)		5.58E + 07	3.13E + 07	7.15E + 07	6.86E + 07
VNNYC$_{[mbbr]}$VDC$_{[IAM]}$EETSK		2.93E + 08	1.81E + 08	5.42E + 08	3.58E + 08
VNNYC$_{[mbbr]}$VDC$_{[mbbr]}$EETSK	β955	5.52E + 07	2.32E + 07	6.98E + 07	4.19E + 07
VNNYC$_{[IAEDANS]}$VDC$_{[mbbr]}$EETSK (22–28%)		2.14E + 07	8.96E + 06	1.93E + 07	1.31E + 07
GNTLTQC$_{[IAM]}$LGFQEFQK	β1159	3.72E + 08	2.33E + 08	4.99E + 08	4.90E + 08
GNTLTQC$_{[mbbr]}$LGFQEFQK		1.61E + 09	9.98E + 08	1.98E + 09	1.69E + 09
AAEIDC$_{[IAM]}$QDIEER	β1544	8.59E + 07	5.75E + 07	1.59E + 08	1.26E + 08
AAEIDC$_{[IAEDANS]}$QDIEER		5.77E + 08	3.47E + 08	5.14E + 08	5.96E + 08
AAEIDC$_{[mbbr]}$QDIEER		2.01E + 09	1.09E + 09	2.22E + 09	2.09E + 09
EQEVSAAWQALLDAC$_{[IAM]}$AGR	β1883	1.62E + 07	8.13E + 06	4.62E + 07	2.86E + 07
EQEVSAAWQALLDAC$_{[IAEDANS]}$AGR		3.39E + 08	3.17E + 08	2.83E + 08	3.72E + 08
EQEVSAAWQALLDAC$_{[mbbr]}$AGR		9.50E + 08	7.26E + 08	9.75E + 08	1.01E + 09

Ion-flux data of mass-spectometry detected peptides. The raw mass spectrometry ion-flux data Φ_{time} and φ_{time} were calculated from the ratio of IAM and mBBr/IAEDANS peptides in (**A**) α-spectrin and (**B**) β-spectrin. When multiple peptides for the same cysteine were detected, peptides with the greater ion-flux values (bold) were used for analysis. In a majority of cases, less abundant peptides make up less than a third of the total pool.

Table S4. Cys-labeling ratios for ankyrin peptides quantified by mass spectrometry

Peptide	Cys	Repeat	$\Phi_{30'}$	$\Phi_{60'}$	$\varphi_{30'}$	$\varphi_{60'}$
TKDELTPLHCAAR	274	R8	0.88	1.56	0.67	1.26
NGLSPIHMAAQGDHLDC$_{mBBr}$VR (100%)	316	R9	—	—	—	—
AKDDQTPLHC$_{IAEDANS}$AR (100%)	472	R14	—	—	—	—
LCQDYDTIGPEGGSLR	1022	N/A	—	—	1.61	1.76
FWLSDCPR (100% IAM)	1212	N/A	—	—	—	—

The detected Cys peptides for ankyrin are listed together with amino acid number (according to Uniprot accession no. Q02357), repeat, Φ_{time} and φ_{time} (modified/unmodified ion-flux ratios for IAEDANS and mBBr). Ankryrin repeats consist of two alpha helices separated by β-loop turns, and the borders for ankyrin repeats were defined according to Uniprot entry Q02357. Although spectrin repeats fold into independent, protease resistant structures (1), the same cannot be said for ankyrin repeats, despite their labeling as individual domains. Three cysteines, Cys 316 and 472 were only detected in the modified form; therefore Φ_{time} and φ_{time} were not calculated for these peptides. The modification is listed in the peptide sequence, Cys-274-IAEDANS and Cys-472-mBBr were not detected. Cys 1212 was only detected in the unmodified form, and the zero Φ_{time} and φ_{time} values shown as dashes.

1. Kahana E, Marsh PJ, Henry AJ, Way M, Gratzer WB (1994) Conformation and phasing of dystrophin structural repeats. *J Mol Biol* 235:1271–7.